

Growth and Characterization of CdSe_{1-y}S_y Nanofilms Obtained by Chemical Bath Deposition

J. I. Contreras-Rascón · J. Díaz-Reyes ·
R. S. Castillo-Ojeda · J. A. Balderas-López ·
J. S. Arias-Ceron · J. E. Flores-Mena

Received: 10 May 2014 / Published online: 22 October 2014
© Sociedade Brasileira de Física 2014

Abstract In this work, the growth and characterization of cadmium selenide sulphur (CdSe_{1-y}S_y) deposited by chemical bath deposition (CBD) technique at the reservoir temperature of 20±2 °C are presented, varying the thiourea volume added to the growth solution in the range of 0–30 ml. The films chemical stoichiometry was determined by energy-dispersive X-ray spectroscopy (EDS). The X-ray diffraction (XRD) analysis and Raman scattering reveal that CdSe_{1-y}S_y-deposited films showed hexagonal wurtzite crystalline phase. The average size of the crystalline grain in relation to the sulphur volume varies in the range of 1.48–9.2 nm that was determined by using the Debye-Scherrer equation for the direction (100), which is confirmed by analyzing the grain average

diameter by high-resolution transmission electron microscopy (HRTEM). Raman scattering shows that the lattice dynamics is characteristic of bimodal behaviour and the multiplex adjustment of the first optical longitudinal mode for the CdSe denotes, in all cases, the Raman shift of the characteristic peak in the range of 177–181 cm⁻¹ of the CdSe crystals associated with the sulphur incorporation. CdSe_{1-y}S_y band gap energy can be varied from 1.86 to 2.11 eV by varying the thiourea volume added in the growth solution measured by transmittance at room temperature.

Keywords Alloys · Electronic materials · Non-crystalline materials · Chemical synthesis · XRD · HRTEM · Raman spectroscopy · Transmittance

J. I. Contreras-Rascón
Universidad del Valle de Puebla, 3 Sur, 5759. Col. El Cerrito, Puebla,
Puebla 72440, México

J. Díaz-Reyes (✉)
Centro de Investigación en Biotecnología Aplicada, Instituto
Politécnico Nacional, Ex-Hacienda de San Juan Molino Km. 1.5,
Tepetitla, Tlaxcala 90700, México
e-mail: joel_diaz_reyes@hotmail.com

R. S. Castillo-Ojeda
Universidad Politécnica de Pachuca, Rancho Luna, Ex-Hacienda de
Santa Bárbara, Zempoala, Hidalgo 43830, México

J. A. Balderas-López
Unidad Profesional Interdisciplinaria de Biotecnología del Instituto
Politécnico Nacional, Av. Acueducto S/N, Col. Barrio la Laguna,
Del. Gustavo A. Madero, México, DF 07340, México

J. S. Arias-Ceron
Centro de Investigación en Dispositivos Semiconductores, ICUAP,
Benemérita Universidad Autónoma de Puebla, CU, Edif. No. 137,
Col. San Manuel, Puebla, Puebla 72570, México

J. E. Flores-Mena
CINVESTAV-IPN, Depto. de Física. Apdo, Postal 14-740, México,
DF 07000, México

1 Introduction

Sulphur cadmium selenide semiconductor (CdSe_{1-y}S_y) crystals are used in the manufacture of photovoltaic and optoelectronic devices [1, 2], since they have a high sensitivity in the near-infrared and visible regions. In addition, compound semiconductor CdSe_{1-y}S_y thin films obtained by chemical bath deposition have low surface activity [3], good photoconductive and photoluminescent properties for the production of photoresistors with light detection capabilities in the spectral region between 1.5 and 3 eV [4]. Chemical bath deposition technique being one of the most useful in the deposition of CdSe_{1-y}S_y nanocrystalline layers for its application in semiconductor gas sensors for the detection of oxygen has attracted interest in recent years due to its potential applications in the protection of the environment, medicine, industry, security, etc. [5].

Various methods of synthesizing semiconductor nanocrystals (NCs) have been investigated in liquid phase, in which NCs are suspended in most organic solvents or

aqueous solution, making them less practical for fabrication and integration into optoelectronic devices. Therefore, the solidification of NCs in matrix is prerequisite before the assembling of NCs into electronic and optoelectronic devices. Recently, hybrid organic/inorganic nanocomposites have attracted considerable interest due to their promising optoelectronic properties and applications. The alloyed and doped NCs are promising in biological and luminescent bifunctional applications [6, 7]. In previous works, the synthesis, basic optical properties and structural characteristics of doped CdSeS NCs have been reported [8, 9], but the time-resolved luminescent properties are not sufficiently investigated.

In this work, we report the synthesis and characterization of CdSe_{1-y}S_y NCs in one step by chemical bath deposition on glass substrate. In particular, the effects of the chemical composition (*y*) on structural and optical properties of the CdSe_{1-y}S_y alloy were studied by X-ray diffraction, high-resolution transmission electron microscopy (HRTEM), X-ray spectroscopy (EDS), Raman scattering and room temperature transmittance.

2 Experimental Details

CdSe_{1-y}S_y films were deposited using the chemical bath deposition (CBD) on substrates of corning glass at a deposited temperature (*T*_d) of 20±2 °C. Deionized water of 20 MΩ was utilized to prepare the aqueous solutions that are conformed by CdCl₂ [0.01 M], KOH [0.1 M], SeC(NH₂)₂ [0.1 M] and NH₄NO₃ [0.1 M]. Systematically, it was adding thiourea (SC(NH₂)₂) [0.2 M]. The selenourea solution was prepared in an argon inert atmosphere, because it is unstable under laboratory conditions and should be maintained at a temperature of 4 °C to avoid its chemical decomposition. Corning glass substrates were chemically treated prior to the deposition, submerged during 24 h in a K₂Cr₂O₇/HCl solution, washed with soapy water, rinsed and finally dried with hot air. Deposit time was 30 min by CBD. Film colour changes from dark brown to dark yellow depending on the thiourea volume added at the grown solution. Films present a mirror-like surface morphology and very good adhesion to the corning glass substrates. The thiourea volume is added systematically during the deposition in volumes of 5 ml, keeping constant the experimental parameters: pH, stirring, volumes, deposited temperature and molar ratios. For carrying out the intentional doping by sulphur of the deposited layers, we added small thiourea amounts to the growth solution in the range of 0 to 30 ml to obtain different sulphur concentrations in the nanofilms. These nanofilms are labelled to differentiate the nanofilm M100 that is binary to M205, M310, M415, M520, M625 and M730 that are ternary nanofilms. The numbers 05, 10, 15, 20, 25 and 30 are referred to the thiourea volume added systematically in growth solution. The chemical stoichiometry of the CdSe_{1-y}S_y samples was studied by

EDS that was carried out in a system LEO 438VP, with W.D. of 26 mm using a pressure of 20 Pa. The crystalline phase and structure of the films were determined with a Bruker D8 Discover diffractometer using the copper Kα radiation ($\lambda=1.5406$ Å) at 40 kV and 40 mA with parallel beam geometry. HRTEM studies were carried out in a JEOL JEM200 of 80–200 kV. The obtained image is recorded with a CCD camera in real time. The Gatan Digital Micrograph software was used for the analysis of HRTEM images. Raman scattering experiments were performed at room temperature using the 6,328 Å line of a He–Ne laser at normal incidence for excitation. The light was focused to a diameter of 6 μm at the sample using a ×50 (numerical aperture 0.9) microscope objective. The nominal laser power used in these measurements was 20 mW. Care was taken to avoid the heating of the sample inadvertently to the point of changing its Raman spectrum. Scattered light was analyzed using a micro-Raman system (Lambram model of Dilor), a holographic notch filter made by Kaiser Optical System, Inc. (model SuperNotch Plus), a 256×1,024-pixel CCD used as detector cooled to 140 K using liquid nitrogen and two interchangeable gratings (600 and 1,800 g/mm). Typical spectrum acquisition time was limited to 60 s to minimize the sample heating effects discussed above. Absolute spectral feature position calibration to better than 0.5 cm⁻¹ was performed using the observed position of Si which is shifted by 521.2 cm⁻¹ from the excitation line. The transmittance measurements were performed using a Bruker Infrared Spectrometer Vertex 70 at room temperature.

3 Experimental Results and Discussion

Figure 1a shows X-ray patterns of CdSe_{1-y}S_y nanofilms with different sulphur concentrations deposited at a temperature of 20±2 °C. It is observed from XRD patterns that CdSe_{1-y}S_y films deposited are polycrystalline in nature, which show a preferential growth in the (002) direction, besides other peaks observed in the (110) and (112) directions. It can be seen that each peak corresponds fairly well with the data of CdSe_{1-y}S_y marked in the software DICVOL04 data. The obtained structural parameters with the software DICVOL04 data are in good agreement with the published ones. From this close agreement, it is confirmed that as deposited CdSe_{1-y}S_y thin films for all the thiourea concentrations belong to the hexagonal wurtzite crystal system. The X-ray patterns of deposited CdSe_{1-y}S_y thin films are described in the *P63mc* (186) and whose lattice parameters were calculated using the software DICVOL04, obtaining the following lattice parameters values: *a*=4.215 and *c*=6.872 Å, which are in agreement with the reported values [10]. In all cases, the samples present the same reflections and can be assigned directly. Besides, a widening at the peak of the preferential (002) direction, which could be caused by undergoing stress, size of small crystalline

domain or fluctuations in concentration, was observed. The first case does not happen since the substrate is amorphous, and it does not produce a mismatch in the lattice parameters. The variation in the average size of the crystalline domain is the cause of this widening. In fact, to apply the Debye-Scherrer equation [11], one finds that the crystalline domain increases. The mean grain size was calculated from hexagonal wurtzite (002) reflection of $\text{CdSe}_{1-y}\text{S}_y$, for the all the studied samples. Figure 1b shows the deconvolution of X-ray diffractograms of the samples M100 and M720 that are undoped film and the film with 30 ml of thiourea. These results show that the grain size increases as the thiourea concentration is increased in the growth solution as can be observed in Table 1.

Figure 2 shows the variation of the size of the average crystalline domain with the sulphur incorporation obtained by the Debye-Scherer equation through the measurement of the full width at half maximum (FWHM) of the more intense peak that is (002) direction of deposited layers, which is sited about 25.499° . The intensity of this peak depends lightly of the sulphur molar fraction in the thin films. Figure 3 illustrates an image obtained by HRTEM for a typical sample, M730, and the insert is the result of the processing of the HRTEM image using filters in Fourier space. There is a crystal structure of nearly spherical shape of the material with an average size of ~ 7.3 nm, and in addition, in the insert, it can be seen clearly the distance interplanar of material which corresponds to the direction of the hexagonal phase of the CdSeS (001). As can

be seen, the results obtained by HRTEM are in good agreement with the results calculated from X-ray diffraction.

The chemical composition of the samples is analyzed by EDS, which besides allows to know the presence of any unintentional impurities, which were not detected by X-ray diffraction. The EDS spectra indicate the presence of oxygen in the samples along with cadmium, selenium and sulphur [11] (see Fig. 4). However, these oxygen ions can form trap levels in the band gap, resulting in several transitions contributing to luminescence. Thus, it appears that oxygen has replaced sulphur or selenium at a few random points of the $\text{CdSe}_{1-y}\text{S}_y$ lattice. Figure 4a shows the bulk EDS spectrum of the CdSe nanostructure grown with zero S molar fractions, which indicates that besides Cd and Se, the sample contains a significant amount of sodium, silicon and oxygen. Figure 4b shows the typical bulk EDS spectrum of the sample $\text{CdSe}_{1-y}\text{S}_y$ sample grown with the maximum thiourea concentration. This sample contains a large amount of cadmium and sulphur, besides a significant amount of oxygen that can form CdO. The results of such measurements for the cadmium, selenium and sulphur are shown in Table 1. From these results, it is observed that the samples do not have a good stoichiometry and that they have a greater presence of cadmium in the material and an absence of sulphur and selenium. Continuing with the consideration that each unit cell contains two zinc atoms and two sulphur and selenium atoms, then when a stoichiometric deviation of ideal unit cell occurs, it could establish a correspondence between vacancies or

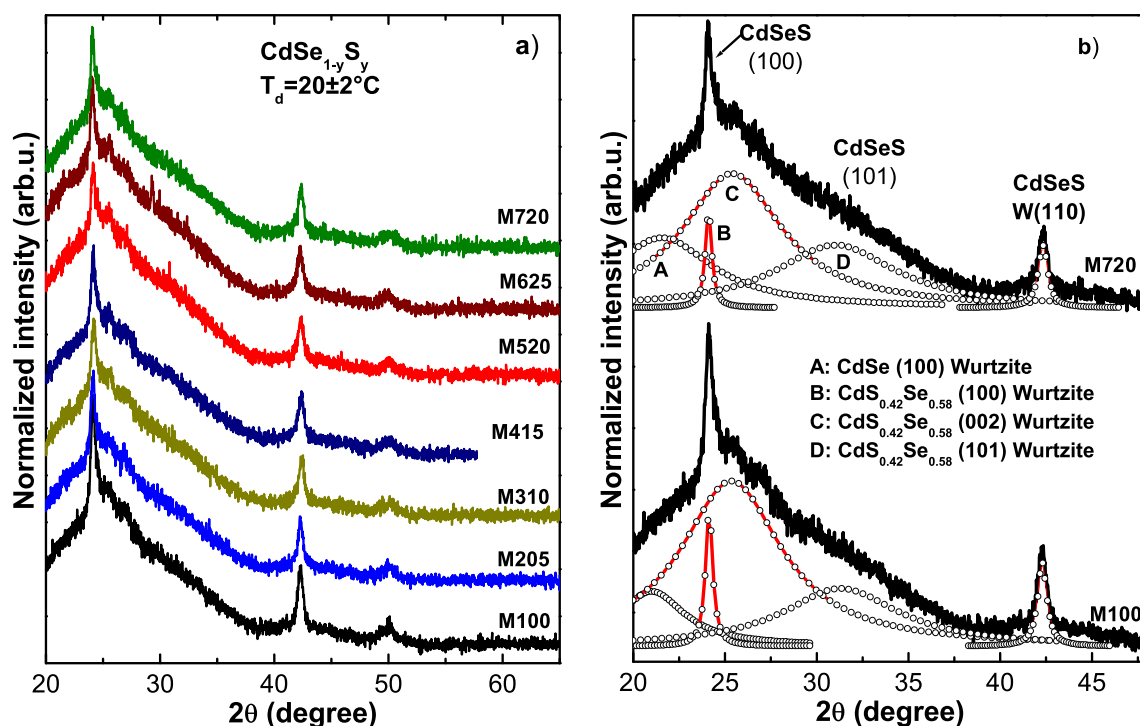


Fig. 1 **a** X-ray patterns of $\text{CdSe}_{1-y}\text{S}_y$ nanofilms with different sulphur concentrations deposited at a temperature of $20 \pm 2^\circ\text{C}$. **b** Deconvolution of X-ray diffractograms of two samples: M100 and M720

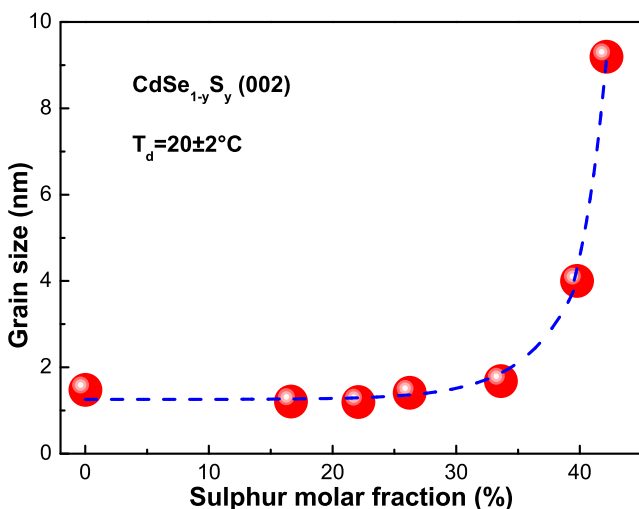
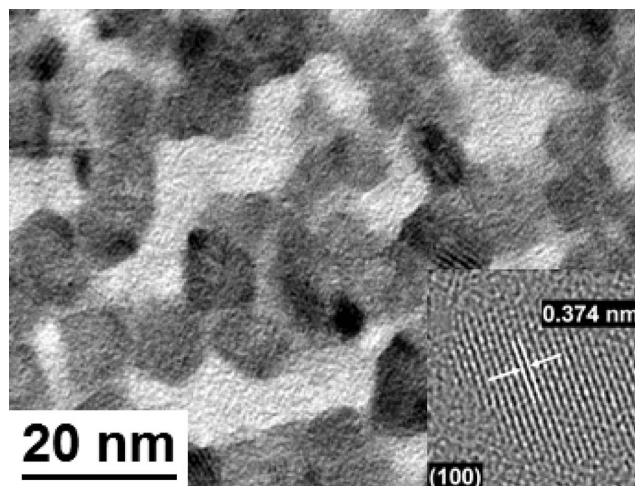
Table 1 Summary of the CdSe_{1-y}S_y samples studied in this work and the doping volume added to each one

Sample	SC(NH ₂) ₂ added volume (ml)	Cd molar fraction	Se molar fraction	S molar fraction	Grain size (nm)
M100	00	49.11	50.89	0.0	1.481
M205	05	56.40	22.06	21.54	1.206
M310	10	57.72	20.20	22.08	1.199
M415	15	55.54	21.46	23.00	1.407
M520	20	53.76	12.62	33.62	1.686
M625	25	55.76	4.46	39.78	4.000
M730	30	55.48	2.39	42.13	9.200

The Cd, Se and S concentrations in CdSe_{1-y}S_y samples were measured by means of energy-dispersive spectroscopy (EDS). Besides, the mean grain sizes of the nanostructures are obtained by the Debye-Scherrer equation for the direction (002)

interstices of some of the elements (V_{Cd} , V_{Se} , V_S , Cd_i , Se_i , S_i). From Table 1, one observes that the samples contain a lower sulphur and selenium concentration, which indicates that they have a higher structural defect concentration. This is the case of the present work, where there are excess of II element and lack of VI elements.

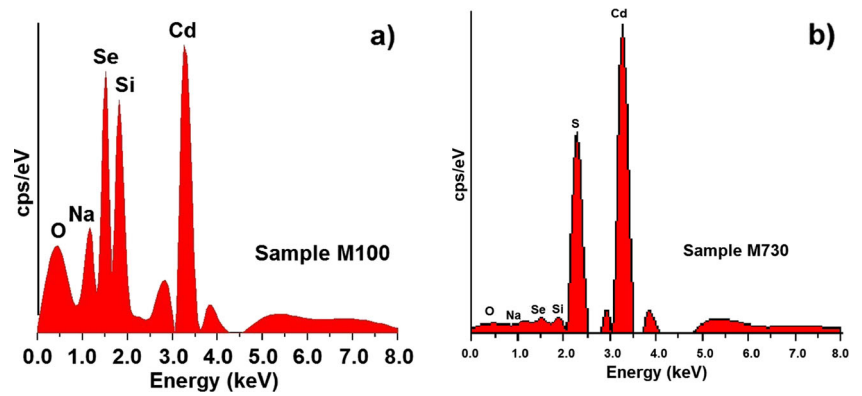
Back scattering geometry has been used to record the Raman spectra of CdSe and CdSe_{1-y}S_y that are shown in Figs. 5 and 6. CdSe Raman spectrum features an asymmetric fundamental Raman band at around 208 cm⁻¹ that can be fitted well with the sum of three Lorentzian lines. The most prominent mode at 208 cm⁻¹ corresponds to the first-order CdSe longitudinal optical phonon (1LO-CdSe) in hexagonal wurtzite phase [12, 13], and the mode corresponding to the low-energy shoulder originates from surface optical (SO) phonon modes at 183 cm⁻¹ [14, 15]. The feature at the high-energy shoulder, sited at 237 cm⁻¹, is the subject of a recent study by Dzhagan et al. [16], who suggest that it results from

**Fig. 2** Dependence of the grain size of the average crystalline domain based on the increase of sulphur molar fraction for the CdSe_{1-y}S_y system**Fig. 3** HRTEM micrograph of a typical CdSeS sample, M730

the participation of acoustic phonons to the scattering process. The band sited at 415 cm⁻¹ is associated to the second longitudinal optical mode of the CdSe (2LO-CdSe) [13]. There is a vibrational band at 371 cm⁻¹ that is associated with 2SO [17]. On the other hand, the bands around 400 and 600 cm⁻¹ are overtones of the fundamental Raman band. Finally, the band at 624 cm⁻¹ corresponds to 3LO-CdSe [17].

Figure 6 displays the CdSe_{1-y}S_y alloys Raman spectra deposited on corning glass with different sulphur molar fractions in the growth solution, which present mainly the similar Raman bands of that CdSe. Figure 7 shows the Raman spectra of the samples M205 and M730, which were grown with lower and higher thiourea volumes that present the same form of the CdSe Raman spectrum. Raman spectrum of the sample M730 can be deconvoluted in six Lorentzian line shape signals as shown in Fig. 7, which are located at 187, 209, 272, 377, 417 and 601 cm⁻¹. Using the same procedure described above for assigning the vibrational bands, the most prominent mode at 209 cm⁻¹ is observed near at frequency of 1LO-CdSe which is associated to the first-order CdSe longitudinal optical phonon-like (CdSe-1LO-like) band, although its Raman shift does not depend on the sulphur concentration in the layer. In the same way, the Raman mode corresponding to the low-energy shoulder (187 cm⁻¹) originates from SO phonon modes, and the feature at the high-energy shoulder, sited at 272 cm⁻¹, is the subject of a recent study but is notorious in its Raman shift at higher frequencies. The band sited at 417 cm⁻¹ is associated to the second longitudinal optical mode-like band of the CdSe (CdSe-2LO-like) [13]. Finally, the modes located at 377 and 601 cm⁻¹ correspond to the second and third phononic replica of the SO mode, 2SO and 3SO, respectively. The intensity of the CdSe-1LO-like and CdSe-2LO-like bands decreases with the increase of thiourea compound concentration, as can be seen in Fig. 8, and this effect will be explained in the following lines. From Fig. 6, it is seen that not only the first-order 1LO Raman line is broadened, but also it

Fig. 4 Bulk EDS spectra of $\text{CdSe}_{1-y}\text{S}_y$ typical samples: **a** M100 and **b** M730 samples. The spectra indicate that besides Cd, Se and S, the samples contain a significant amount of oxygen



shows an asymmetric broadening towards the low-frequency side. It is found from Fig. 7 that the position of these LO-like peaks does not undergo any Raman shift by the thiourea volume increase in the samples, but their FWHMs have decreased noticeably compared to that of the M205 sample FWHM. It is now well known that confinement of phonons, optical and acoustic, influences the phonon spectra conspicuously when the grain size falls to a few nanometres. Confinement of optical phonons causes an asymmetry in the line shape and a shift towards the low-frequency side compared to that of bulk CdSe. In bulk crystals, the phonon eigenstate is a plane wave and the selection rule for Raman scattering is $q \approx 0$, where q is the wave vector. But, in

nanocrystallites, the spatial correlation function of the phonons is finite due to the phonon confinement, and hence, $q \approx 0$ selection rule is relaxed and Raman signals from the phonon branch away from the zone centre also contribute to the resultant Raman line. The net effect of this contribution is the development of a marked asymmetry of the Raman line towards the low-frequency side. Quantitative descriptions of the effect of phonon confinement on the Raman spectra of nanostructured materials have been reported by different researchers [18, 19].

The samples used for transmission measurements were deposited on corning glass substrates of 100 μm of thickness.

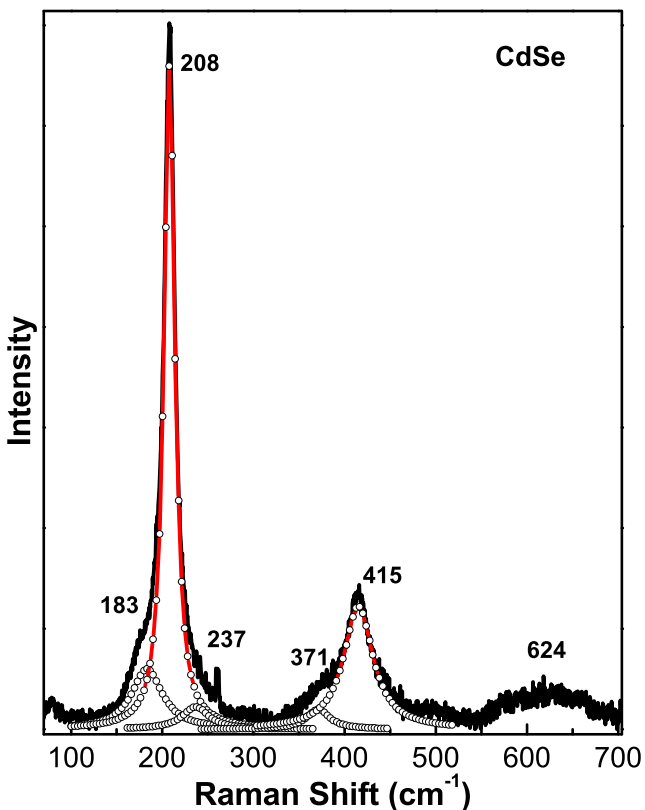


Fig. 5 CdSe Raman spectrum

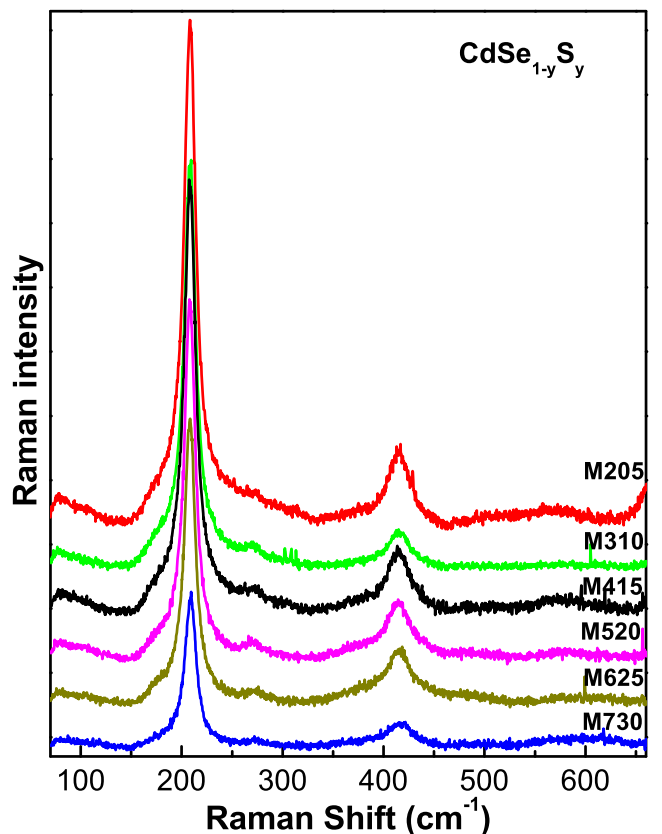


Fig. 6 Raman spectra of the $\text{CdSe}_{1-y}\text{S}_y$ films by adding different sulphur volumes deposited at the temperature of 20 ± 2 °C

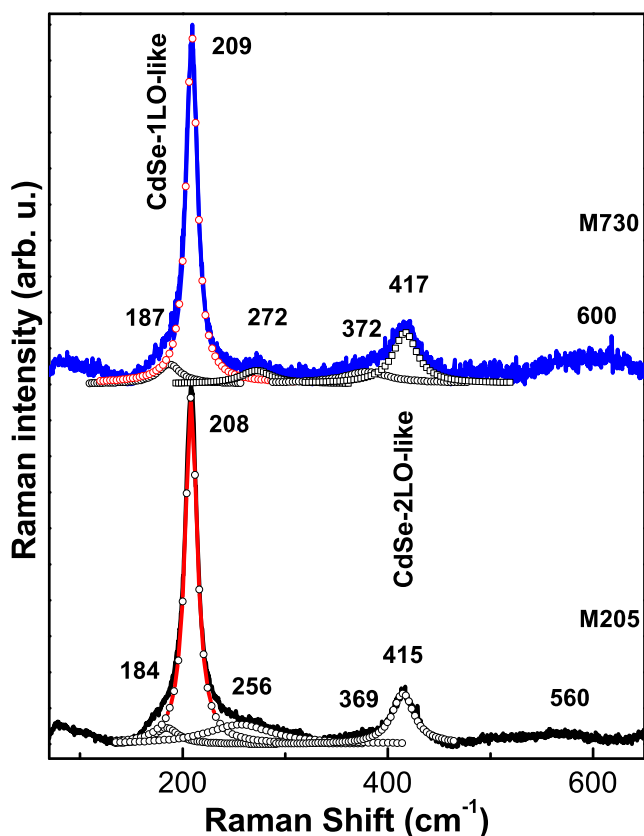


Fig. 7 Decomposition of the measured Raman spectra into individual components (Lorentzian shape) for two molar fractions: a sample M205 and b sample M730. The dashed lines are their respective fitting

The transmittance spectra in the visible and infrared ranges were recorded for the CdSe_{1-y}S_y thin films in the wavelength range 400–1,100 nm. The effects of sulphur incorporated in the layers on the optical properties including percentage of transmittance (% of T) and energy band gap (E_g) are studied in detail. Figure 9 shows the transmission spectra of CdSe_{1-y}S_y films prepared at 20±2 °C temperature on corning glass. The

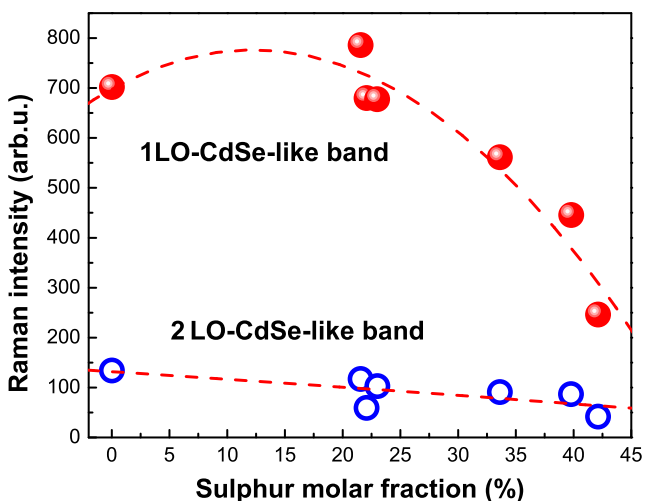


Fig. 8 Intensity variation of the two dominant bands in the Raman spectra

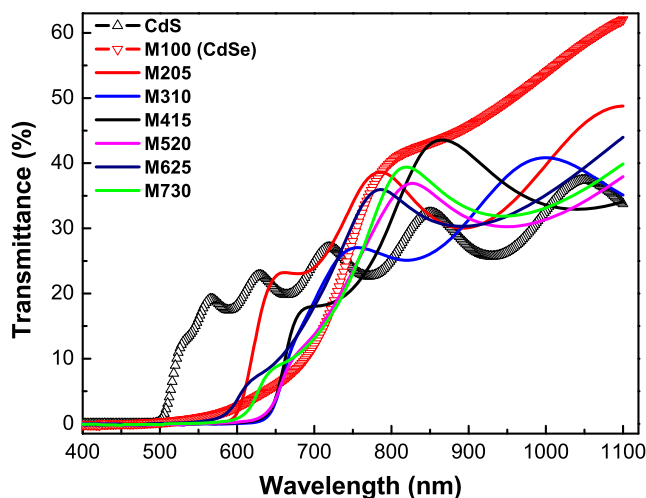


Fig. 9 Transmittance spectra of CdSe_{1-y}S_y nanofilms

observed transmittance of the CdSe film in the visible range varies from about 0 up to nearly 60 % (without considering the substrate contribution), and it is the highest of all shown transmittance spectra. The sharp reduction in the transmittance spectrum at the wavelengths lower than 600 nm is due to the fundamental absorption edges of the different films. The CdSe films were transparent, with no observable blue colouration under our experimental conditions. The transmittance of the CdSe_{1-y}S_y films decreases slightly, as can be seen in Fig. 9. The decrease in transparency of the CdSe_{1-y}S_y films with an increase of the sulphur molar fraction is caused by the slight increase in the band gap energy, which confirms the formation of CdSe_{1-y}S_y (see Fig. 10). It is observed from the transmittance spectra that the absorption edge is also slightly shifted towards the higher-energy region for the films with higher sulphur molar fraction.

The intrinsic absorption edge of the films can be evaluated and discussed in terms of the indirect interband transition. The

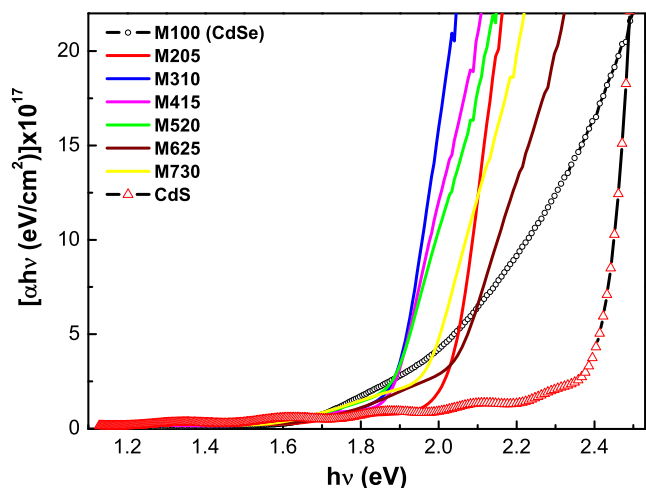


Fig. 10 Band gap energy determination of CdSe_{1-y}S_y nanofilms at room temperature

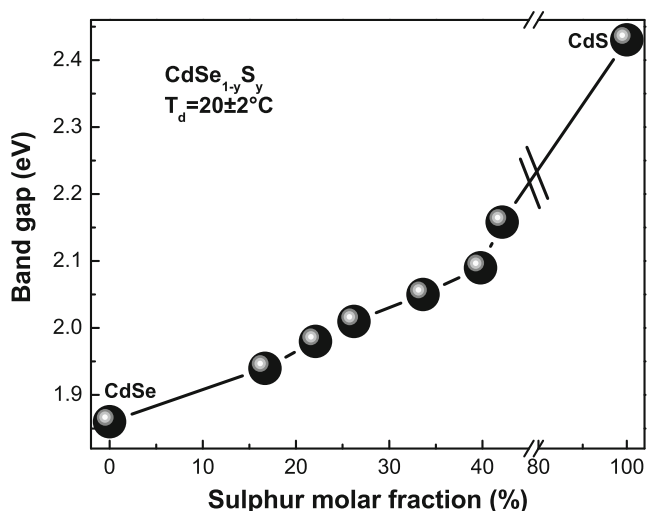


Fig. 11 Band gap energy as a function of the sulphur molar fraction. The band gap energies of the binary compounds, CdSe and CdS, are shown

optical band gap energy (E_g) was evaluated from the absorption coefficient (α) using the standard relation: $(\alpha h\nu)^{1/2} = A(h\nu - E_g)$ is expected to show a linear behaviour in the higher-energy region, which should correspond to a strong absorption near the absorption edge. Extrapolating the linear portion of this straight line to zero absorption edge gives the optical band gap energy, E_g , of the films which are shown in Fig. 11. The absorption coefficient α for a film of thickness d and reflectance R was determined near the absorption edge using the simple relation: $\alpha = \ln\{(1-R)^2/T + [(1-R^2)/2T]^2 + R^2\}^{1/2} / d$, where multiple reflections are taken into consideration, but interference neglected, and d is the film thickness. Actually, a transmission interference pattern could be observed in most samples and was used to get an accurate value for the thickness d . The optical band gap energy for the CdSe is calculated at about 1.86 eV that corresponds to pure CdSe band gap in the bulk. In order to take into account the samples added with sulphur, the optical band gap is increased slightly by about 0.31 eV, which can be related to sulphur incorporation to the molecule, as can be seen in Fig. 11. This band gap increase can be explained because the substitution in the lattice of selenium atoms by sulphur atoms is smaller.

4 Conclusions

In this work, the growth and characterization of CdSe_{1-y}S_y ternary thin films obtained by CBD technique were presented under our proposed reactant species and 20 ± 2 °C as deposited temperature. The results of the X-ray diffraction and Raman spectroscopy studies showed that the obtaining NCs belongs

to hexagonal wurtzite crystal system and the cation effect in the CdSe_{1-y}S_y ternary compounds is used to modify the optical band gap energy. The mean grain sizes of the nanocrystals are in the range 1.48–9.2 nm, which were determined using the Debye-Scherrer equation for the direction (100), that indicate a high quantum confinement, which were confirmed by HRTEM. Raman scattering showed that the lattice dynamics is characteristic of bimodal behaviour and the multipeak adjust of the first optical longitudinal mode for the CdSeS denotes in, all cases, the Raman shift of the characteristic peak in the range of 177–181 cm⁻¹ of the CdSe nanocrystals associated with sulphur. CdSe_{1-y}S_y band gap energy can be varied from 1.86 to 2.11 eV by varying the sulphur molar fraction in the grown nanofilms measured by transmittance at room temperature.

References

1. M.A. Contreras, A.M. Gabor, A.L. Tennant, A. Asher, J.R. Tuttle, R. Noufi, *Prog. Photovolt.* **2**, 287 (1994)
2. T.B. Tang, *J. Electron. Math.* **4**, 1229 (1975)
3. C.S. Ferekides, K. Dugan, IEEL 1st WCPEC, Dec. 5–9, Hawaii (1994) 99
4. G. Gordillo, *Sol. Energ. Math. Sol. C.* **25**, 41 (1992)
5. Z. Aneva, D. Nesheva, C. Main, S. Reynolds, A.G. Fitzgerald, *Semicond. Sci. Technol.* **23**, 095002 (2008)
6. S.A. Santangelo, E.A. Hinds, V.A. Vlaskin, P.I. Archer, D.R. Gamelin, *J. Am. Chem. Soc.* **129**, 3973 (2007)
7. W.C. Kwak, T.G. Kim, W.S. Chae, Y.M. Sung, *Nanotechnology* **18**, 205702 (2007)
8. D.Q. Yu, X. Chen, H.Q. Zhang, L.Z. Hu, J.C. Sun, S.S. Qiao, K.T. Sun, J.X. Zhu, *Sci. Chin.: Phys. Mech. Astron.* **53**, 1842 (2010)
9. J.Y. Ouyang, M. Vincent, D. Kingston, P. Descours, T. Boivineau, M.B. Zaman, X.H. Wu, K. Yu, *J. Phys. Chem. C* **113**, 5193 (2009)
10. U. Hotje, C. Rose, M. Binnewies, *Solid State Sci.* **5**, 1259 (2003)
11. J.I. Contreras-Rascon. (2013). Ph. D. Thesis centro investigación en dispositivos semiconductores. Benemerita Universidad Autonoma de Puebla
12. R. Beserman, M. Balkanski, *Phys. Rev. B* **1**, 608 (1970)
13. M. Hayek, O. Brafman, *Int Conf. on light scattering in solids*, Paris (1971) 76
14. F. Comas, N. Studarta, G.E. Marquesa, *Solid State Commun.* **130**, 477 (2004)
15. H. Lange, M. Artemyev, U. Woggon, C. Thomsen, *Nanotechnology* **20**, 045705 (2009)
16. V.M. Dzhagan, I. Lokteva, M.Y. Valakh, O.E. Raevska, J. Kolny-Olesiak, D.R.T. Zahn, *J. Appl. Phys.* **106**, 084318 (2009)
17. N. Tschirner, H. Lange, A. Schliwa, A. Biermann, C. Thomsen, K. Lambert, R. Gomes, Z. Henz, *Chem. Mater.* **24**, 311 (2012)
18. H. Richter, Z.P. Wang, L. Ley, *Solid State Commun.* **39**, 625 (1981)
19. H. Campbell, P.M. Fauchet, *Solid State Commun.* **58**, 739 (1986)